Circular Motion Geometry by Minimal 2 Points in 4 Images

Guang JIANG[1,3], Long QUAN[2], and Hung-tat TSUI[1]
[1]Dept. of Electronic Engineering, The Chinese University of Hong Kong, New Territory, Hong Kong
[2]Dept. of Computer Science, Hong Kong University of Science and Technology, Kowloon, Hong Kong
[3]School of Technical Physics, Xidian Univeristy, Xi'an 710071, P.R.China
{gjiang,httsui}@ee.cuhk.edu.hk, quan@cs.ust.hk

Abstract

This paper describes a new and simple method of recovering the geometry of uncalibrated circular motion or single axis motion using a minimal data set of 2 points in 4 images. This problem has been solved using non-minimal data either by computing the fundamental matrix and trifocal tensor in 3 images, or by fitting conics to tracked points in 5 images. Our new method first computes a planar homography from a minimum of 2 points in 4 images. It is shown that two eigenvectors of this homography are the images of the circular points. Then, other fixed image entities and rotation angles can be straightforwardly computed. The crux of the method lies in relating this planar homography from two different points to a homology naturally induced by corresponding points on different conic loci from a circular motion. The experiments on real image sequences demonstrate the simplicity, accuracy and robustness of the new method.

1. Introduction

Acquiring 3D models from circular motion sequences, particularly turntable sequences, has been widely used by computer vision and graphics researchers. Generally, the whole reconstruction procedure includes the determination of camera positions at different viewpoints, detection of object boundaries and extraction of surface models from a volume representation. The estimation of the camera positions or simply the rotation angles relative to a static camera is the most important and difficult part of the modelling process. Traditionally, rotation angles are obtained by careful calibration [14, 18, 19]. Fitzgibbon et al. [7] extended the single axis approach to recover unknown rotation angles from uncalibrated image sequences based on a projective geometry approach. In this method, corresponding points are tracked from each pair of images for the fundamental matrices and from each triplet of images for the trifocal tensors. Jiang et al. [11] tracked 2 points in at least 5 images from uncalibrated image sequences to fit 2 conics and then from the conics to recover images of circular points and rotation angles. Another interesting paper is proposed by Mendonça et al. [13] who recovered the rotation angles from profiles of surfaces under the calibrated image sequence.

However, by counting the invariant quantities under the circular motion, it is evident that in none of the existing methods are the parameters minimal. In this paper, we propose a new minimal method that requires only 2 points in 4 images. Further, our algorithm is remarkably simple. First we estimate a homography from the 8 points, then calculate the eigenvectors of this 3×3 transformation to obtain the invariant quantities. The advantage of this new method over existing methods is straightforward. First, it uses the minimal data set of 2 points in 4 images, while the existing ones need at least 7 points for the fundamental matrix and trifocal tensor or need 2 points in 5 images. Second, the calculation is in a closed-form solution obtained by only solving a real cubic equation.

The paper is organized as follows. Section 2 reviews work on invariants under the circular motion. Section 3 presents the method of calculating these invariants using 2 points in 4 views. Analysis and proof of the result are given in Section 4. A RANSAC method is presented in Section 5 to choose the most reliable points and optimize the results. Section 6 demonstrates two experiments to verify this method. A short conclusion is presented in Section 7.

2. Review of circular motion and its associated fixed image entities

Circular motion or single axis motion consists of a set of Euclidean actions such that the relative motion between a scene and a camera can be described by rotations about a single fixed axis. The most common case is a static camera that views an object rotating on a turntable with fixed internal parameters [14]. The equivalent case is when an object is fixed and the camera rotates around. This a particular case of the more general planar motion [1, 4] as it restricts all motion to rotation around a single axis. Without loss of

Proceedings of the Ninth IEEE International Conference on Computer Vision (ICCV 2003) 2-Volume Set
0-7695-1950-4/03 $17.00 © 2003 IEEE

generality, we assume that the rotation axis is vertical as the z-axis of the world coordinates and the camera is moving on the horizontal plane.

The fixed image entities of the circular motion are similar to the planar motion, which include two lines. One is the image of the rotation axis $\mathbf{l}_s$. Note that $\mathbf{l}_s$ is a line of fixed points. Unlike in planar motion, the line $\mathbf{l}_s$ is fixed in all images under circular motion. The other line is called the horizon line $\mathbf{l}_h$. It is the vanishing line of the horizontal plane. Unlike the image of the rotation axis, the horizon line is a fixed line, but not a line of fixed points. Since the image of the absolute conic ω is fixed under rigid motion, there are two points, which are at the intersection of the image of the absolute conic ω with the line $\mathbf{l}_h$. They remain fixed in all images. Actually, these two fixed points are the image of the two circular points on the horizontal planes. These fixed image entities of the circular motion are illustrated in Figure 1[11].

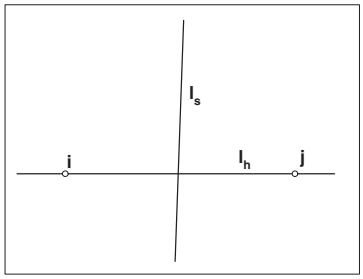

Figure 1. Fixed image entities under circular motion.

Since the line $\mathbf{l}_h$ is determined by the images of circular points, there are in total 6 d.o.f. which is enough to determine the fixed entities of the circular motion. There are 2 for each of image of the two circular points and 2 for images of the rotation axis $\mathbf{l}_s$.

3. Minimal method using 2 points in 4 images

Under circular motion, the trajectory of one space point is a circle and this circle projects to a conic in the image plane. Each of such conics can be fitted by the corresponding points in five images. It has been shown in [11] that two such conics are enough to recover these fixed entities of circular motion. The determination of two conics is equivalent to a total of 10 points in image, they count for $2\times5\times2=20$ degrees of freedom as each point has 2 d.o.f. in image. After subtracting the 6 d.o.f. fixed entities of circular motion and 6 d.o.f. of the two points in space, the 8 d.o.f. remaining are the rotation angles associated with all images involved. As the 10 tracked points can spread at most over 2 different groups of 5 images, the 8 d.o.f. remaining can be counted for the 4 rotations angles of each group of 5 images. The case of two conics is therefore minimal for this particular case of 2 groups of 10 images. But it is redundant in any other cases. For instance, for a common case that the two points are tracked over the same 5 images, it is highly redundant as only 4 parameters needs to be determined from the 8 given ones.

Motivated by the above redundancy of the existing methods [7, 11], we propose a minimal solution using only 2 points in 4 images in this section. Analysis and proofs of the results will be given in the next section.

1. Given 2 points tracked over 4 images $\mathbf{a}_i$ and $\mathbf{b}_i$ for $i = 1\ldots4$, compute a 3×3 plane homography $\mathbf{H}$ such that $\lambda\mathbf{b}_i = \mathbf{H}\mathbf{a}_i$. This can be easily solved by a SVD method with normalized image coordinates [9].
2. Compute the eigenvalues and eigenvectors of the homography $\mathbf{H}$. As $\mathbf{H}$ is a 3×3 matrix, this is equivalent to solving a cubic equation with real coefficients. By the circular motion constraint, two of the eigenvalues are a pair of conjugate complex numbers. The corresponding pair of complex conjugate eigenvectors is the image of the pair of circular points $\mathbf{i}$ and $\mathbf{j}$.
3. The horizon line is determined by $\mathbf{l}_h = \mathbf{i}\times\mathbf{j}$.
4. Each point is tracked over 4 image points, and its conic locus also goes through the images of the circular points. These two sets of 4 points $\mathbf{a}_i$ and $\mathbf{b}_i$ can be fitted to conics $\mathbf{C}_p$ and $\mathbf{C}_q$ respectively with 2 images of the circular points $\mathbf{i}$ and $\mathbf{j}$ on the conic.
5. Once we obtained the conics, the following steps are the same as those described in [11]. We briefly summarize as follows:

   The pole of each conic with respect to the the horizon line $\mathbf{l}_h$ is given by $\mathbf{o}_p = \mathbf{C}_p^{-1}\mathbf{l}_h$, and $\mathbf{o}_q = \mathbf{C}_q^{-1}\mathbf{l}_h$. They are the images of the center of the two space circles, and lie on the image of the rotation axis $\mathbf{l}_s$. The rotation axis can be calculated as $\mathbf{l}_s = \mathbf{o}_p \times \mathbf{o}_q$.

   The rotation angles related to these four images can be calculated by using Laguerre's formula [17, 5], $\theta_{mn} = \frac{1}{2i}\log(\{\mathbf{l}_{o_pa_m}, \mathbf{l}_{o_pa_n}; \mathbf{l}_{o_pi}, \mathbf{l}_{o_pj}\})$, where $m, n = 1\ldots4$.

It is interesting to notice that solving a cubic equation is reminiscent of similar situations in self-calibration using both a special trifocal tensor [1] and a 1D trifocal tensor [4]. But the trifocal tensor needs many more points to be determined, 6 points in 3 images, but here only 2 points in 4 images.

4. Analysis of the homography H

In this section, we will give a detailed analysis of the planar homography we have introduced from 2 points tracked in 4 images.

4.1. Existence of the homography H

Figure 2(a) shows two conics that are fitted by corresponding points of two space points in different images. The intersections of these two conics include one pair of complex conjugate points, which are the images of the circular points and lie on the horizon line $\mathbf{l}_h$. Obviously, each conic is the image of a circle on a space plane on which the space point moves. With the transforms of translation, scale and rotation, the two circles can be mapped to a unit circle with its center as the origin[11] on space plane π_s. If we have four points on these two conics respectively, these two sets of points can be mapped to the same four points on the unity circle since they have the same relative angles (Figure 2(b)).

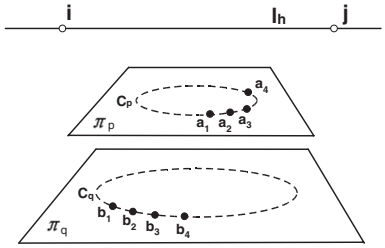

(a)

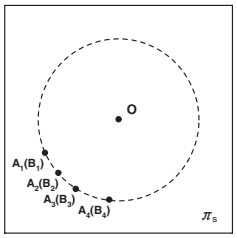

(b)

Figure 2. The existence of a planar homography with respect to the 2 points in 4 images. (a) Two sets of points lie on two horizontal planes; points $\mathbf{a}_i$ and $\mathbf{b}_i$ are corresponding points under the homography H. (b) These two sets of points can be mapped to the same four points on a unit circle with its center as the origin.

If we set the planar homography of plane π_p and plane π_q with respect to plane π_s as $\mathbf{H}_{ps}$ and $\mathbf{H}_{qs}$, respectively, it is clear that there is a planar homography between plane π_p and plane π_q that is determined by the 2 points in 4 images.

$$\mathbf{H} = \mathbf{H}_{ps}^{-1}\mathbf{H}_{qs}. \tag{1}$$

4.2. Homology $\mathbf{H}_{pq}$

The planar homography $\mathbf{H}$ reflects a special relationship between plane π_p and plane π_q. Let's first examine a more direct homological relationship between these two planes.

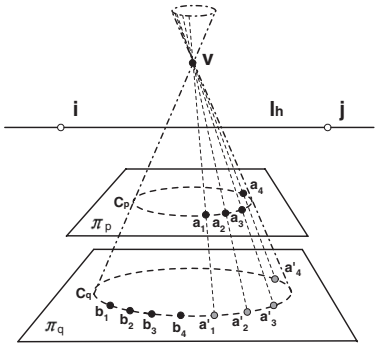

(a)

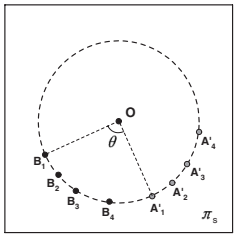

(b)

Figure 3. The analysis of the homography. a) A homology constrained by the two conics, points $\mathbf{a}_i$ and $\mathbf{a}'_i$ are corresponding points under the homology $\mathbf{H}_{pq}$. (b) These two sets of points $\mathbf{a}_i$ and $\mathbf{a}'_i$ can be mapped to two sets of four points on a unit circle with its center at the origin and the same relative rotation angles.

Two circles on parallel planes can determine two double-cones. Figure 3(a) shows one of them where the vertex is located on the same side of the circles. The second double-cone has the vertex located between the two circles. It is easy to see that the vertex always lies on the image of the rotation axis. A point correspondence between the two conics $\mathbf{C}_p$ and $\mathbf{C}_q$ can be established by drawing lines from the vertex. For instance, from the line connecting vertex $\mathbf{v}$ and point $\mathbf{a}_1$, we get corresponding points $\mathbf{a}_1$ and $\mathbf{a}'_1$. This is known to be a homology, a special projective transformation that transforms a conic into another one. This homology also leaves a point and a line fixed [17, 10]. For single axis motion, the fixed line of the homology is the horizon line $\mathbf{l}_h$ and the fixed point is the vertex $\mathbf{v}$. This homology $\mathbf{H}_{pq}$ can be parameterized [10] as

$$\mathbf{H}_{pq} = \mathbf{I} + (\mu - 1)\frac{\mathbf{v}\mathbf{l}_h^T}{\mathbf{v}^T\mathbf{l}_h} \tag{2}$$

Proceedings of the Ninth IEEE International Conference on Computer Vision (ICCV 2003) 2-Volume Set
0-7695-1950-4/03 $17.00 © 2003 IEEE

where $\mathbf{I}$ is the identity matrix, and μ the characteristic invariant of the planar homology. The geometric interpretation of the characteristic μ is the cross ratio of the vertex $\mathbf{v}$, any corresponding homological points , and the intersection point of the connected line of the corresponding points with $\mathbf{l}_h$.

4.3. The relationship between homography and homology

First, the homology $\mathbf{H}_{pq}$ relates the points $\mathbf{a}_i$ on the conic $\mathbf{C}_p$ to the points $\mathbf{a}'_i$ on the conic $\mathbf{C}_q$ for $i = 1, \ldots, 4$. Second, a rotation $\mathbf{R}(\theta)$ relates the points $\mathbf{a}'_i$ to the points $\mathbf{b}_i$ on the space plane for $i = 1, \ldots, 4$. Hence, the composition of the homography is given by

$$\mathbf{H} = \mathbf{H}_{qs}^{-1}\mathbf{R}(\theta)\mathbf{H}_{qs}\mathbf{H}_{pq}, \tag{3}$$

where $\mathbf{H}_{qs}$ maps the plane π_q to the Euclidean plane π_s (see Figure 3(b)).

4.4. Eigenvectors of H

Now, we prove the main result that the image of the circular points are the eigenvectors of the homography $\mathbf{H}$ associated with the pair of complex conjugate eigenvalues.

- We first consider the special case when the θ is not equal to 0 or π and when the μ is equal to 1. In this case, the two circles lie on one same plane and the homology is the identity matrix:

  $$\mathbf{H} = \mathbf{H}_{qs}^{-1}\mathbf{R}(\theta)\mathbf{H}_{qs}. \tag{4}$$

  The eigenvalues of $\mathbf{R}(\theta)$ are 1, and a pair of complex conjugates $e^{\pm i\theta}$. The eigenvectors corresponding to the pair of conjugate complex eigenvalues are the circular points $(1, \pm i, 0)^T$. The transformation $\mathbf{H}_{qs}^{-1}\mathbf{R}\mathbf{H}_{qs}$ is a similar matrix of $\mathbf{R}$. Therefore it keeps the eigenvalues, but transforms the eigenvectors into the images of the circular points $\mathbf{H}_{qs}^{-1}(1, \pm i, 0)^T$.

- The most general case is when θ is not equal to 0 or π, and μ is different from 1. As the images of the circular points lie on the line $\mathbf{l}_h$, from equations 2 and 3, the homology leaves the image of the circular points invariant. This proves that the eigenvectors corresponding to the pair of complex conjugate eigenvalues are generally the images of the circular points.

- The homography $\mathbf{H}$ is degenerated to the homology $\mathbf{H}_{pq}$ when $\theta = 0$. When $\theta = \pi$, it is equivalent to the case where the vertex of the double-cone is located between two circles, and $\theta = 0$. Then, $\mathbf{H}$ is also degenerated to a homology $\mathbf{H}_{pq}$.

  $$\mathbf{H} = \mathbf{H}_{pq} = \mathbf{I} + (\mu - 1)\frac{\mathbf{v}\mathbf{l}_h^T}{\mathbf{v}^T\mathbf{l}_h}. \tag{5}$$

  Clearly, the real eigenvalue 1 is repeated twice. As the corresponding eigenvectors are points on $\mathbf{l}_h$. We can not distinguish the value of the images of the circular points when these 8 points satisfy a homology. This degenerate case can be easily detected by its geometric construction: the four lines connecting the corresponding points meet at the vertex point.

4.5. Analysis of the degrees of freedom

The minimal data set of 2 points in 4 images are used to recover the geometry of circular motion in our new method. Each point has 2 d.o.f. in the image plane and 3 d.o.f. in 3D space. These 8 points can determine $2 \times 4 \times 2 - 2 \times 3 = 10$ degrees of freedom, which correspond to the images of the circular points (2×2 d.o.f.), the image of rotation axis (2 d.o.f.), the characteristic invariant μ (1 d.o.f.) and three rotation angles related to these four images (3 d.o.f.).

The planar homography $\mathbf{H}$ is a concatenation of four matrices. The planar homology $\mathbf{H}_{pq}$ has 5 degrees of freedom, where the vertex $\mathbf{v}$ has 2 d.o.f., the axis $\mathbf{l}_h$ has 2 d.o.f. and the characteristic invariant μ has 1 d.o.f.. The matrix $\mathbf{H}_{qs}$ only maps the point on the image plane to a Euclidean plane. This matrix can be parameterized using only the two images of circular points[12, 11]. These two images of circular points have 4 d.o.f.. However, since the line $\mathbf{l}_h$ has been considered in matrix $\mathbf{H}_{pq}$, the matrix $\mathbf{H}_{qs}$ only has 2 d.o.f.. The matrix $\mathbf{R}(\theta)$ has 1 d.o.f.. In total, there are 8 degrees of freedom of the planar homography $\mathbf{H}$.

5. Robust optimization using RANSAC

The minimal solution can be easily plugged into an optimization procedure in which we can remove the tracking outliers. In this section, we describe a complete optimization procedure using RANSAC[6].

1. Arrange the data set S.

   The tracking data are structured into a quadruplet of the image coordinates $\{\mathbf{x}_1, \mathbf{x}_2, \mathbf{x}_3, \mathbf{x}_4\}$ for each point tracked in 4 images. Note that it is unnecessary to assume that the 4 images are consecutive.

2. Compute the fixed image entities with the new method using 2 points in 4 images.

   Randomly select 2 points in 4 images from the data set S, compute the homography. First check if the homography is a homology, then compute the fixed image entities, the images of the circular points $\mathbf{i}$ and $\mathbf{j}$, the image of rotation axis $\mathbf{l}_s$, and the horizon line $\mathbf{l}_h$.

3. Calculate the evaluation value $\mathcal{C}_{\mathbf{x}}$ for each correspondence in 4 images from the data set S.

   First, a conic can be fitted to the 4 points plus 2 points that are the image of the circular points by SVD. Then,

an approximate point-conic distance is defined to be [2, 15, 10]

$$d(\mathbf{x}, \mathbf{C})^2 = \sum_{i=1}^{4} \frac{(\mathbf{x}_i^T \mathbf{C} \mathbf{x}_i)^2}{4((\mathbf{C}\mathbf{x}_i)_1^2 + (\mathbf{C}\mathbf{x}_i)_2^2)},$$

where $(\mathbf{Cx})_m$ denotes the m-th component of the 3-vector $\mathbf{Cx}$.

In addition to the fact that the image of the circular points goes through the conic, there exists also a constraint $\mathbf{C}^{-1}\mathbf{l}_h\mathbf{l}_s = 0$. To take this into account, we compute the following point-line distance:

$$d(\mathbf{l}_s, \mathbf{o})^2 = \frac{(\mathbf{l}_s^T \mathbf{o})^2}{(\mathbf{l}_s)_1^2 + (\mathbf{l}_s)_2^2},$$

where $\mathbf{o}$ is the normalized pole of the $\mathbf{l}_h$ w.r.t. the fitted conic $\mathbf{C}$, and $(\mathbf{l}_s)_m$ is the m-th component of the 3-vector $\mathbf{l}_s$.

The evaluation value $\mathcal{C}_\mathbf{X}$ for each correspondence in 4 images w.r.t. the current fixed image entities is defined to be

$$\mathcal{C}_\mathbf{X} = d(\mathbf{x}, \mathbf{C})^2 + \lambda d(\mathbf{l}_s, \mathbf{o})^2, \qquad (6)$$

where λ can be the Lagrange multiplier.

4. Compute the percentage of inliers consistent with the selected 2 points in 4 images using the threshold evaluation criterion $\mathcal{C}_\mathbf{X}$ by T.

5. Repeat from step 2 to step 4 N times to choose the 2 points in 4 images with the largest number of inliers. N and T are determined by the proportion of inliers [10].

6. Compute an optimal solution using all the inliers. The maximum likelihood estimate is obtained by minimizing $\mathcal{C} = \sum \mathcal{C}_\mathbf{X}$. This nonlinear minimization problem is solved using the Levenberg-Marquart equation from the initial estimates obtained from the minimal data set of 2 points in 4 images.

6. Experiments

The new method of computing circular motion geometry from a minimum of 2 points in 4 images is implemented and tested.

We first set up an experiment to verify the accuracy of the results using the minimal data. Two chessboards are put on a rotary table. Four images of the chessboards shown in Figure 4 are captured at different positions. The positions are chosen to ease the detection of point features as the intersection points of lines. Since the pattern is regular, it is easy to find all corresponding points, 70 points in 4 images. More than 2000 sets of minimal data can be obtained for the computation. We may look at the distribution of the computed coordinates of the image of circular points $(a \pm bi, c \pm di, 1)^T$. A histogram from all sets of data is shown in Figure 5 for each component a,b,c and d. The distribution is without any surprise close to a Gaussian. Most of them are very good results, which means that the minimal data computation is useful in practice to either bootstrap a robust method or an optimization method. There are also some of computed values far away from the peak of the curve. In fact, many of those configurations are close to the degenerate cases of homological points as we discussed in Section 5. This includes two cases: the first is when the intersections of lines connecting corresponding points on the different conics are close to the image of the rotation axis; the second is when the space point is close to the rotation axis.

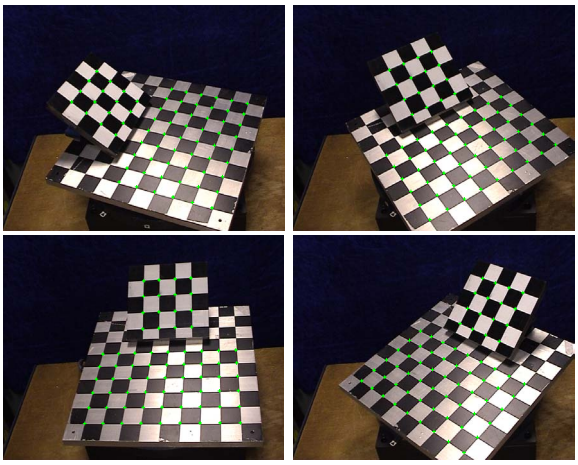

Figure 4. Four test images of the experiment.

Figure 6 shows the recovered horizon line $\mathbf{l}_h$ and the image of rotation axis $\mathbf{l}_s$, from the data sets giving inlier results for a,b,c and d. We should also avoid the case where the rotation planes containing the two points are too close for a stable computation of $\mathbf{l}_s$. The data set automatically selected by RANSAC is also illustrated in Figure 7. The points marked as squares are the minimal data set selected by RANSAC for subsequent optimization. The gray colored points are inliers, and the dark colored points are outliers. Inlier gray colored points are used to fit conics. Optimized solutions are also shown in Figure 5 and Figure 6 with dashed lines.

We also tested our implementation on the popular dinosaur sequence from University of Hannover (obtained from University of Oxford [8]). The sequence contains 36 views from a turntable with a constant angular motion of 10 degrees. The angular accuracy is about 0.05 degrees

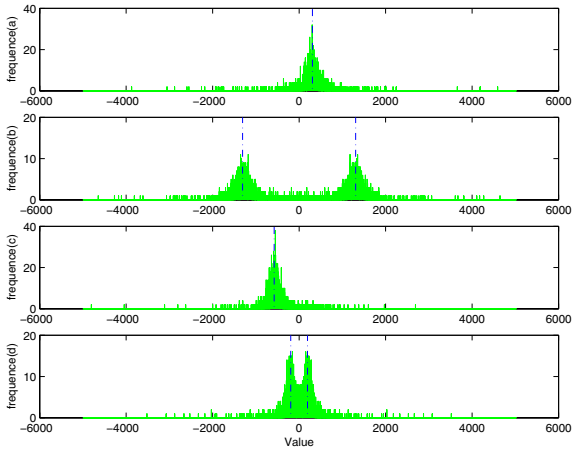

Figure 5. Histogram of a,b,c, and d that are coordinates of the image of circular points $(a \pm bi, c \pm di, 1)^T$. The dashed lines indicated optimized solutions automatically computed.

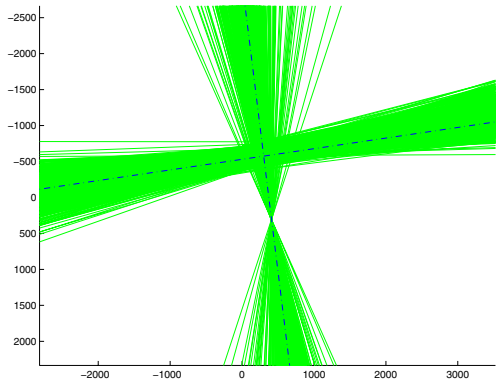

Figure 6. Results of recovered horizon line $\mathbf{l}_h$ and the image of rotation axis $\mathbf{l}_s$ with different minimal data set. The dashed lines are the optimized solutions.

[14]. Figure 8 shows one of the image of the dinosaur sequence and some tracked points along all images. The selected corresponding points are those which have been tracked over at least 4 images separated by long tracking distances. The data set selected by RANSAC marked as squares is shown in Figure 9 in which the gray colored points are inliers and the dark colored points are outliers. The computed results of the images of circular points are $(266.04 \pm 3156.3i, -1151.9 \mp 88.111)^T$. The images of $\mathbf{l}_h$ and $\mathbf{l}_h$ are shown in Figure 10(a). The rotation angles calculated from inlier points are shown in Figure 10(b). If we fix the aspect ratio of the camera and assume a point on the image of rotation axis as a vanishing point [7, 11], the visual hull of the dinosaur can be computed [3, 14]. One view of the 3D model is shown in Figure 11.

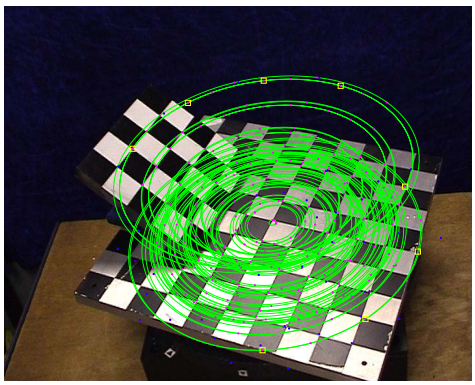

Figure 7. The results computed by RANSAC and optimization. The minimal data set selected by RANSAC are marked in squares. The gray colored points are inliers, and the dark colored points are outliers. These gray colored points are fitted to corresponding conic loci.

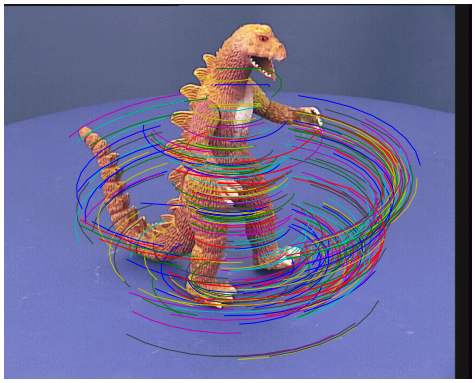

Figure 8. One image of the dinosaur sequence and selected corresponding points.

7. Conclusion

This paper presented a new and simple algorithm of computing the geometry of circular motion or single axis motion using a minimal data set of 2 points in 4 images. This method is minimal compared with existing methods of either using multi-view constraints and conic fitting. The algorithm is also remarkably simple as we only need to compute a 3 by 3 homography, then extract its eigenvalues and eigenvectors. The experiments on real sequences demonstrate the usability of this minimal solution. We also developed a RANSAC driven optimization using initial values provided by this minimal data solution.

Acknowledgments

This project is partially supported by the Hong Kong RGC Grant CUHK 4378/02E and HKUST 6188/02E.

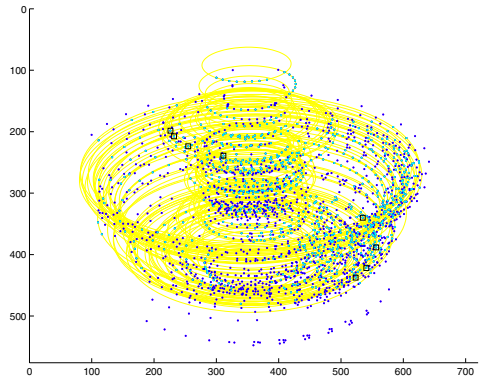

Figure 9. The results computed by RANSAC and optimization. The minimal data set selected by RANSAC are marked in squares. The gray colored points are inliers, and the dark colored points are outliers. These gray colored points are fitted to corresponding conic loci.

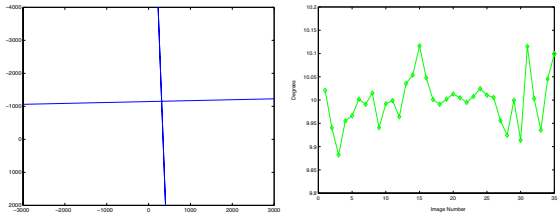

(a) (b)

Figure 10. (a) Image of rotation axis and the horizon line, (b) The computed rotation angles.

Figure 11. 3D reconstruction of dinosaur from silhouettes.

References

[1] M. Armstrong, A. Zisserman, and R. Hartley: Self-Calibration from Image Triplets, *European Conf. on Computer Vision*, pp. 3-16, 1996.

[2] F. Bookstein: Fitting conic sections to scattered data, *Computer Vision, Graphics and Image Processing*, vol. 9, pp. 56-71, 1979.

[3] C.H. Chien and J.K. Aggarwal: Identification of 3D objects from multiple silhouettes using quadtrees/octrees. *Computer Vision, Graphics and Image Processing* 36, 1986, pp.256-273.

[4] O.D. Faugeras, L. Quan and P. Sturm: Self-calibration of a 1D projective camera and its application to the self-calibration of a 2D projective camera, *European Conf. on Computer Vision*, Vol. I, pp. 36-52, 1998.

[5] O.D. Faugeras and Q.T. Luong: Geometry of Multiple Images, *MIT Press*, 2001.

[6] M. A. Fischler and R. C. Bolles: Random sample consensus: a paradigm for model fitting with application to image analysis and automated cartography, *Communication Association and Computing Machine*, 24(6), pp.381-395, 1981

[7] A.W. Fitzgibbon, G. Cross, and A. Zisserman: Automatic 3D Model Construction for Turn-Table Sequences, *European Workshop SMILE'98*, pp. 155-170, 1998.

[8] http://www.robots.ox.ac.uk/ vgg/data/

[9] R. Hartley: In defence of the 8-point algorithm. *IEEE Conf. on Computer Vision*, pp. 1064-1070, 1995.

[10] R. Hartley and A. Zisserman: Multiple View Geometry in Computer Vision, *Cambridge University Press*, 2000.

[11] G. Jiang, H.T. Tsui, L. Quan and A. Zisserman: Single Axis Geometry by Fitting Conics, *European Conf. on Computer Vision*, pp. 537-551. 2002.

[12] D. Liebowitz and A. Zisserman: Metric rectification for perspective images of planes. *IEEE Conf. on Computer Vision and Pattern Recognition*, pp. 482-488, 1998.

[13] P.R.S. Mendonça, K.-Y.K. Wong, and R. Cipolla: Camera pose estimation and reconstruction from image profiles under circular motion. *European Conf. on Computer Vision*, vol. II, pp. 864-877, 2000.

[14] W.Niem: Robust and Fast Modelling of 3D Natural Objects from Multiple Views, *Proc. SPIE*, Vol. 2182, pp. 388-397, 1994.

[15] P.D. Sampson: Fitting conic sections to 'very scattered' data: An iterative refinement of the Bookstein algorithm, *Computer Vision, Graphics and Image Processing*, vol. 18, pp. 97-108, 1982.

[16] H.S. Sawhney, J. Oliensis, and A.R. Hanson: Image Description and 3-D Reconstruction from Image Trajectories of Rotational Motion. *IEEE Trans. on Pattern Analysis and Machine Intelligence*, Vol. 15, No. 9, pp. 885-898, 1993.

[17] J. Semple, and G. Kneebone: Algebraic Projective Geometry. *Oxford University Press*, 1952.

[18] S. Sullivan, and J. Ponce: Automatic model construction, pose estimation, and object recognition from photographs using triangular splines, *IEEE Trans. on Pattern Analysis and Machine Intelligence*, Vol. 20, No. 10, pp. 1091-1097, 1998.

[19] R. Szeliski: Shape from rotation, *IEEE Conf. on Computer Vision and Pattern Recognition*, pp. 625-630, 1991.